Supplemental Figures

Figure S1. Related to Figure 2. Individual-specific cortico-subcortical correlations are reliable with large amounts of data.
(A) We implemented an iterative split-data reliability analysis as in (Laumann et al., 2015; Gordon et al., 2017) on the subcortical voxel-to-cortical network connectivity matrix for each subject and for each subcortical structure (caudate, putamen, pallidum, thalamus), as well as on a cortical vertex-to-cortical network connectivity matrix for each subject for comparison. Reliability reached at least 0.6 (Pearson r) for all subjects for all structures with 100 minutes of motion-censored data, with highest reliability in the caudate. Note that the slopes of the curves do not plateau at 100 minutes, indicating improved reliability may be achieved with even more low-movement data, which exists for most of the MSC subjects. Standard amounts of fMRI data (e.g., 10 minutes) had poor reliability for estimating cortico-subcortical RSFC within an individual. (B) Spatial profile of reliability across voxels was assessed by conducting split-half reliability analyses for each subcortical voxel. Note that in the caudate, reliability was high (> .8) in most voxels in all subjects with very few voxels (< 10% in every subject) having relatively poor reliability (< .5). In the putamen, pallidum, and thalamus, most voxels had reliability > .7 for most subjects. All subsequent analyses excluded voxels with reliability < .5 for each subject, which comprised 14% of voxels on average across subjects (range 6-25%). When these low reliability voxels were included in analyses of integration vs. network-specificity, on average, 45% of them were integrative and 55% were network-specific. Anatomical left is image left.

Supplemental Figures

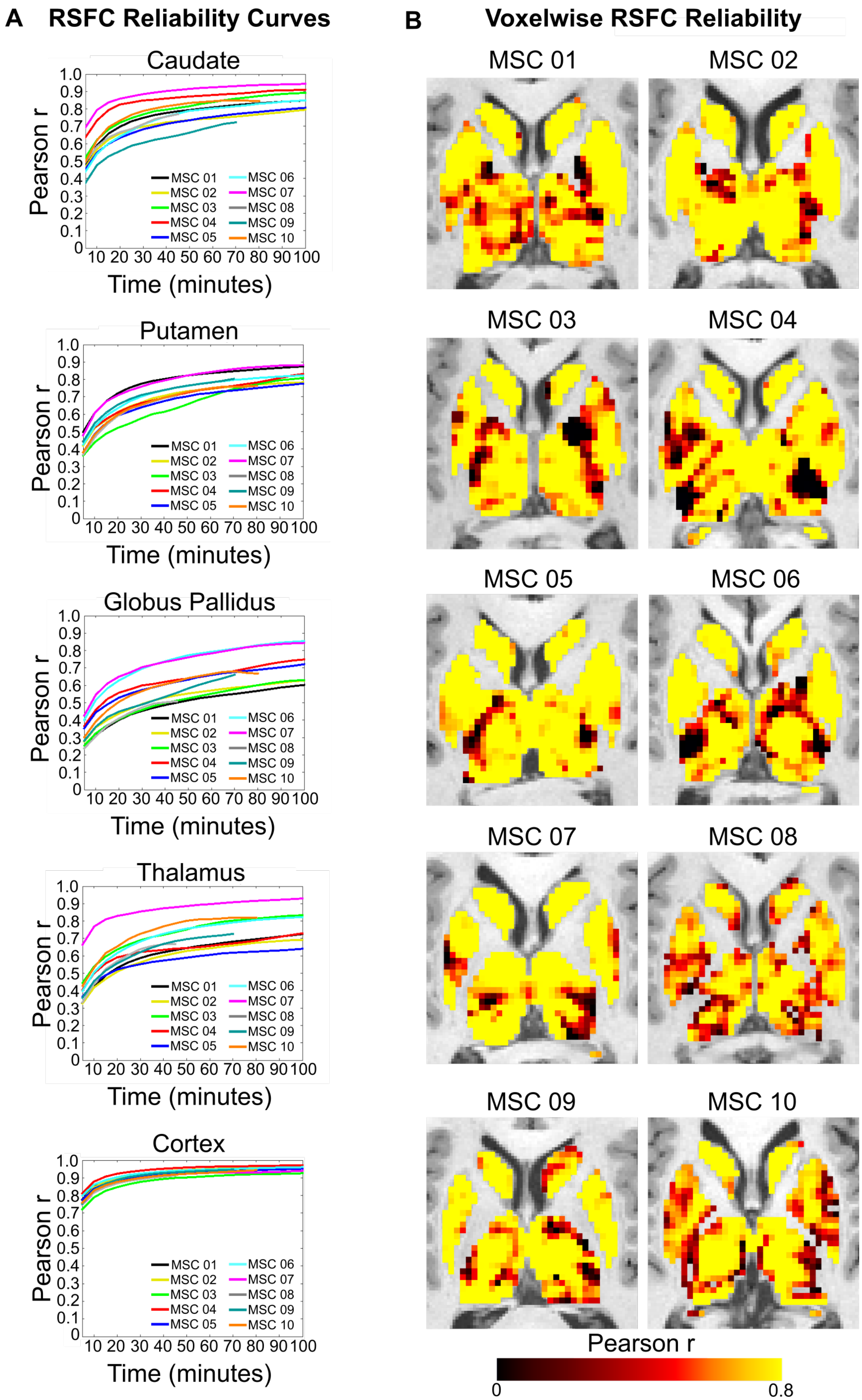

Supplemental Figures

Figure S2. Related to Figure 2. Individual-specific cortico-subcortical RSFC for each network.
For each subject, correlations between subcortical voxels and each cortical network are shown. Anatomical left is image left. VIS = visual; SMH = somatomotor hand; SMF = somatomotor face; CON = cingulo-opercular network; FPN = frontoparietal network; SAL = salience; DAN = dorsal attention network; VAN = ventral attention network; DMN = default-mode network.

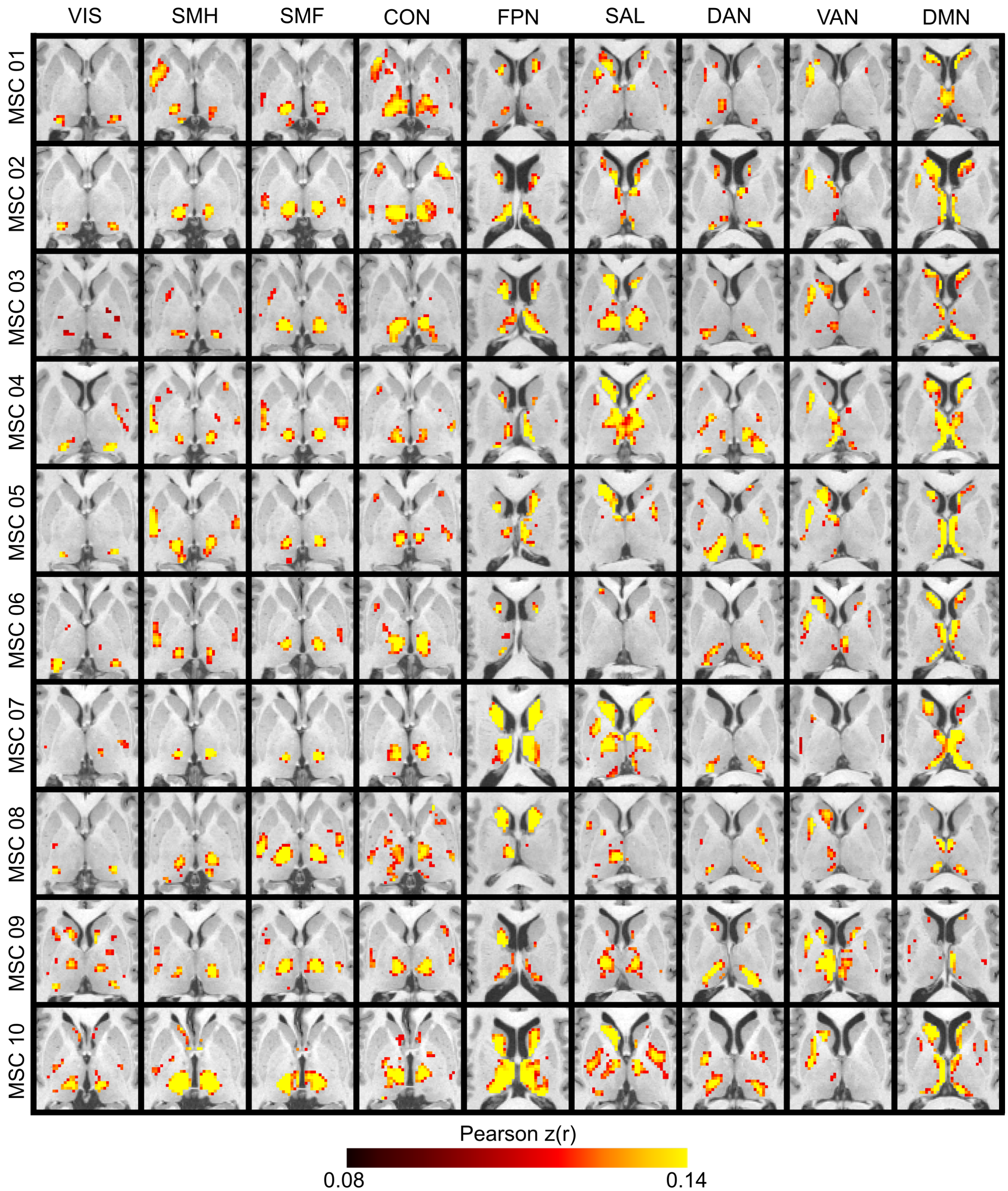

Supplemental Figures

Figure S3. Related to Figure 2. Task/rest overlap for all subjects.
Concordance between RSFC and task activations/deactivations for each individual. Task-evoked increased in BOLD activity during a motor task converge with peak resting-state correlations with the somatomotor hand network. Task-evoked deactivations during a set of cognitive/perceptual tasks converge with peak resting-state correlations with the default-mode network. Anatomical left is image left.

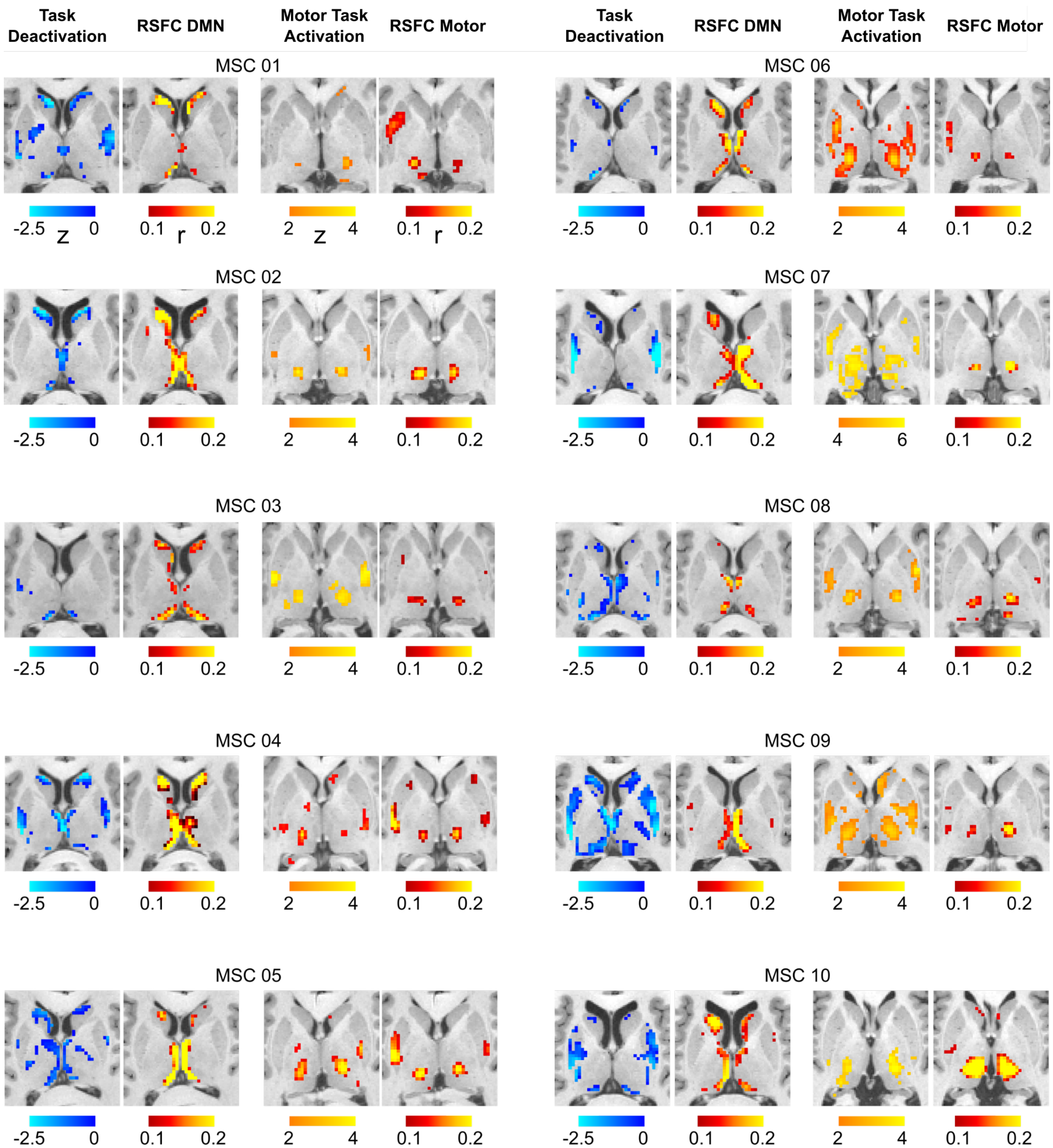

Supplemental Figures

Figure S4. Related to Figure 2. Task activations during the cognitive/perceptual tasks overlapped with multiple cognitive control networks.
Task activations (left panels) are shown for two example subjects next to the modified winner-take-all maps (right panels) for side-by-side comparison. Anatomical left is image left.

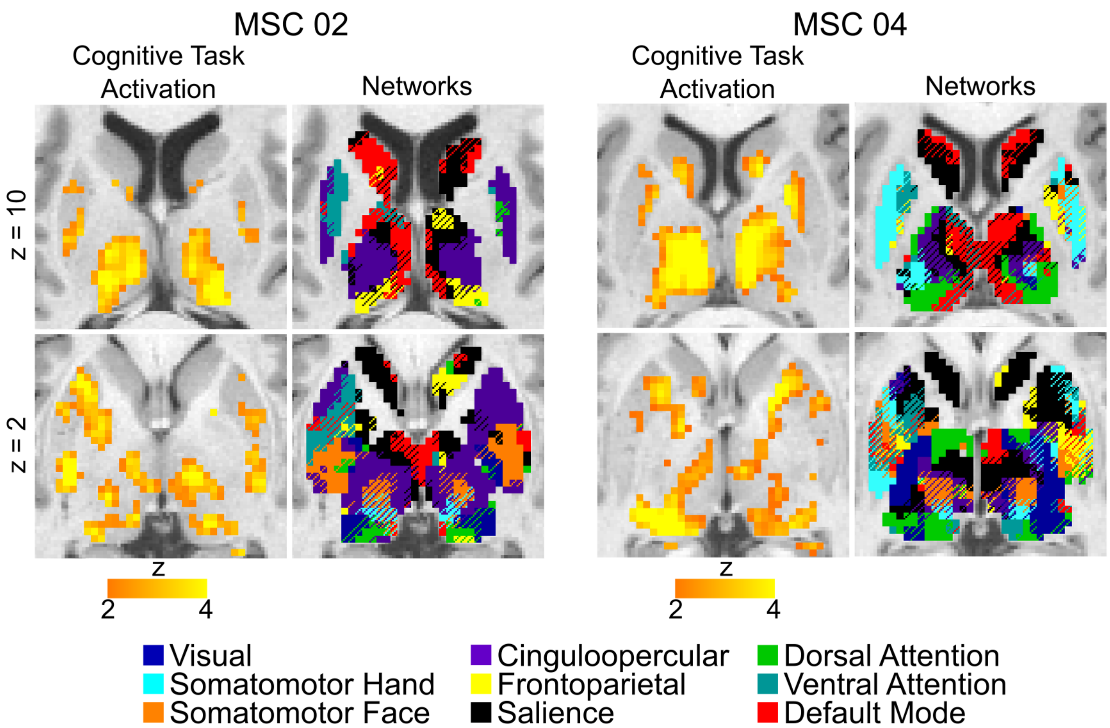

Supplemental Figures

Figure S5. Related to Figure 2. Subcortical network similarity analyses.
Network similarity matrices for the (A) basal ganglia and (B) thalamus. The matrices are organized first by individual and then by split-half sessions (each half represents data from 5 sessions). Off-diagonal elements represent group effects, whereas on-diagonal elements represent individual effects. (C) Quantification of group versus individual effects for RSFC between the basal ganglia and cerebral cortex and between the thalamus and cerebral cortex. On the left, error bars denote standard error of the mean across subjects. On the right, the relative effect magnitudes are plotted as a proportion of the total effects to contrast the relative magnitudes of group and individual effects. Note that an alternative analysis strategy of comparing the standard deviation of the cortico-subcortical correlations between higher-order functional networks (FPN, DAN, VAN, SAL, CON, DMN) and processing networks (VIS, SMH, SMF) confirmed greater variability in the higher-order networks than the processing networks ($t = 13.1$, $p < .001$), and the individual network profiles paralleled that shown here in (C).

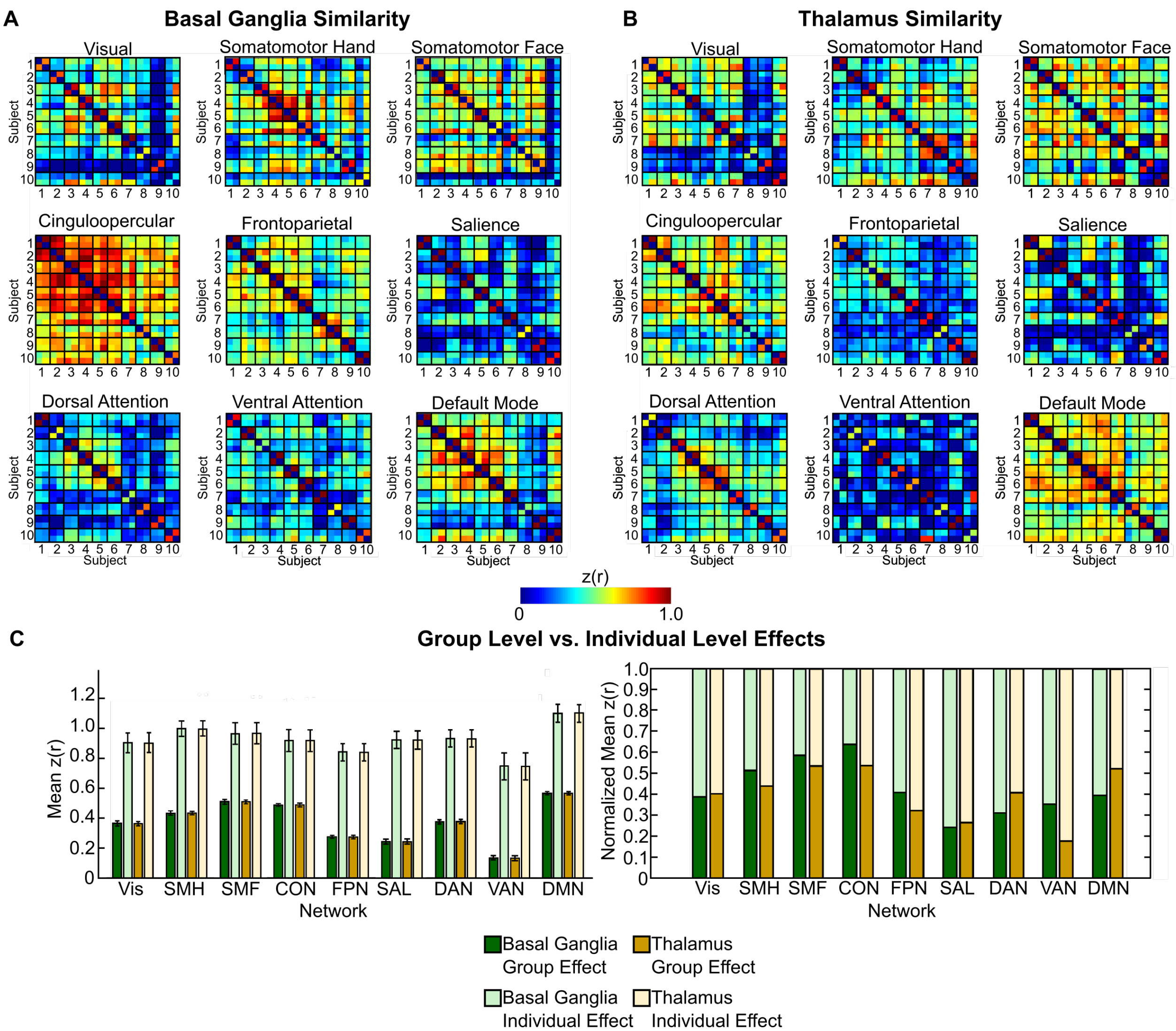

Supplemental Figures

Figure S6. Related to Figure 3. Integrative zone centers were consistent, regardless of the method used to define a voxel as integrative or the specific threshold.
(A) Integrative voxels displayed in black, defined as those in which the correlation with any other network was within a given percent (50%, 66.7%, 75%) of the "winning" network correlation. (B) Integrative voxels displayed in black, defined as those in which the effect size between the correlation with the winning network and another network was less than a given effect size (large, *d*=0.8; medium, *d*=0.5; small, *d*=0.2). Anatomical left is image left.

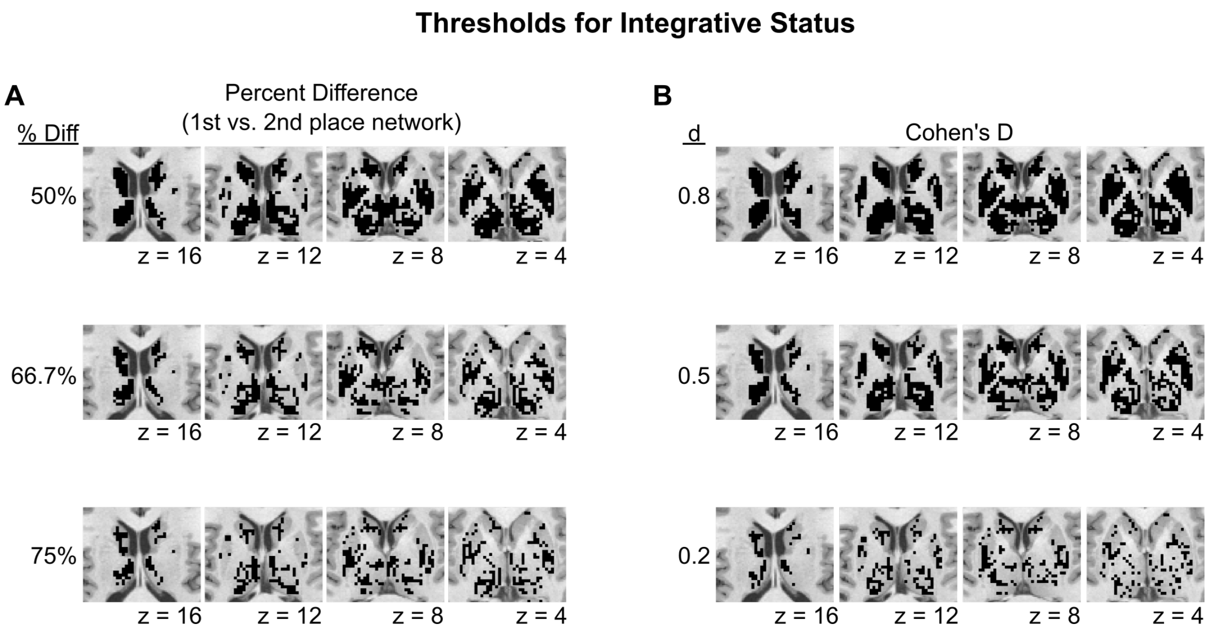

Supplemental Figures

Figure S7. Related to Figure 3. Individual-specific functional organization of the basal ganglia and thalamus.
Voxels with preferential RSFC to one network (network-specific) are represented by solid colors, and voxels functionally connected to multiple networks (integrative) are represented by cross-hatching. Anatomical left is image left.

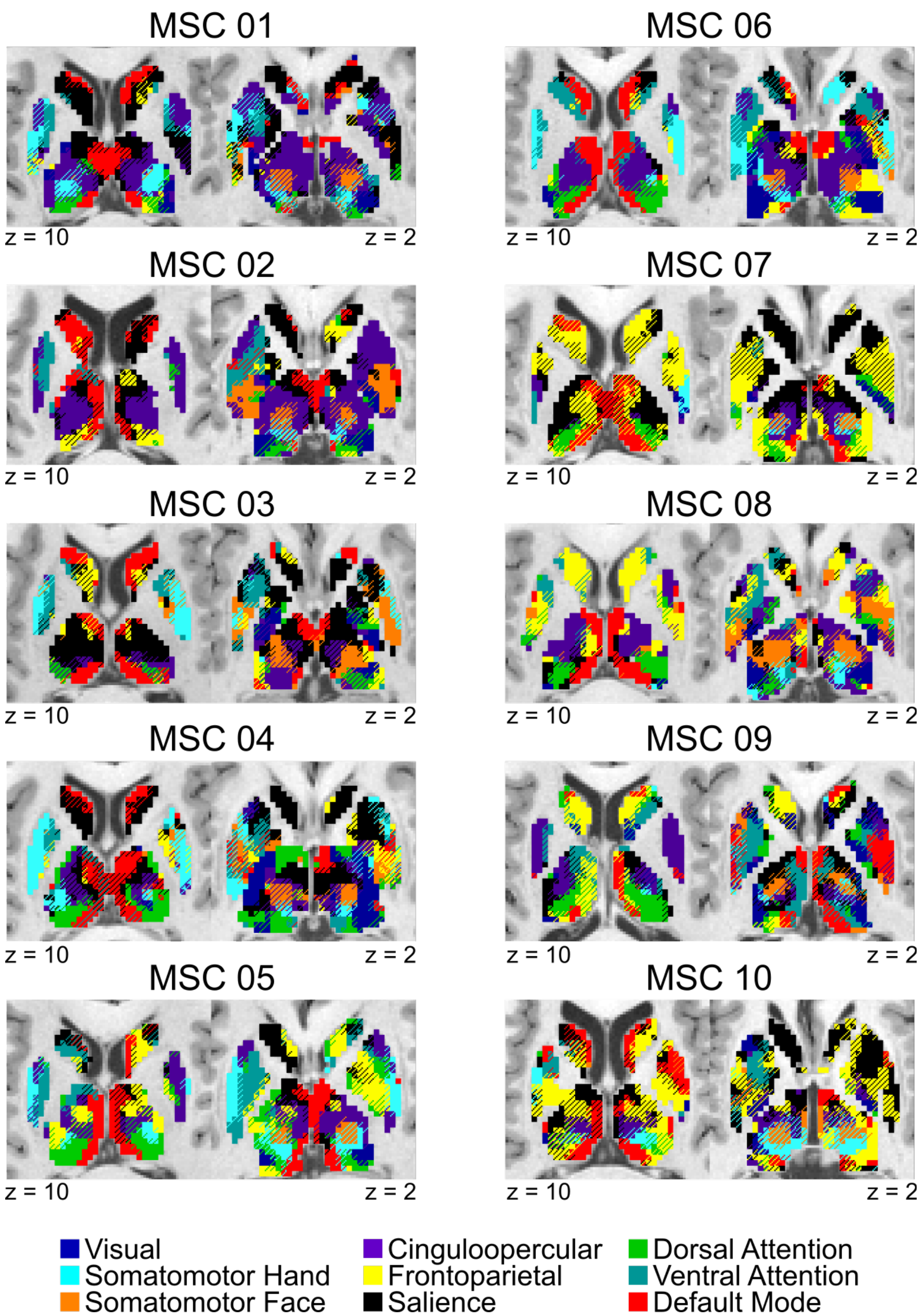

Supplemental Figures

Figure S8. Related to Figure 4 and Figure 5. Integration zones in the subcortex are not driven by the number of *a priori* cortical networks.
The cortical functional networks derived from Infomap are shown on the left for 7-network (A) and 15-network (B) solutions in MSC06. The modified winner-take-all maps in the subcortex (right) are highly similar when using each of these network solutions. The three major integrative zones reported in the main text are consistent across levels of network granularity. For all axial slices, anatomical left is image left.